

# Evaluation of Failure in Low k Films Using Stiffness Mapping and Dynamic Imaging



This article presents the use of dynamic imaging and stiffness mapping on low k materials for analyzing crack lengths in the measurement of fracture toughness and for determining the “finger prints” of failure during scratch testing.

## Introduction

Fracture toughness and scratch failure of thin films on the nanoscale is of particular interest in evaluating film integrity. When conducting fracture toughness tests, crack lengths can be difficult to accurately measure using optical methods or by scanning the topography using a sharp tip as is done with an atomic-force microscope or nanoindenter. These limitations make it common to use a scanning electron microscope for such measurements. A new dynamic scanning technique has now been developed that not only measures topography, but also measures the stiffness of the contact during scanning. This allows fracture and sub-surface effects such as blistering and void formation to be examined. This dynamic imaging technique provides high contrast in areas of fracture due to the abrupt increase in contact area when the tip is physically positioned in the crack and the low stiffness area just removed from the crack due to limited support of surrounding material. This article presents the use of dynamic imaging and stiffness mapping on low k materials for analyzing crack lengths in the measurement of fracture toughness and for determining the “finger prints” of failure during scratch testing.

## Samples

The low k film was a 978nm nanoporous film applied on silicon. The sample was provided by a semiconductor manufacturer in the form of a 150mm wafer. The wafer was diced and mounted to a 1.25-inch sample puck for testing.

## Test Methodology

All testing was conducted using the Nano Indenter® G200 system equipped with the Dynamic Contact Module (DCM), Nano Vision, and Continuous Stiffness Measurement (CSM) options. The DCM transducer is ideal for applications involving ultra-low loads and requiring ultra-high-displacement resolutions. In addition, the higher resonant frequency and lower damping of

this transducer allows higher operating frequencies when scanning to produce stiffness maps. The Nano Vision option enables imaging through the use of a high precision piezo translation stage; lateral resolutions and flatness of travel are better than 2nm. This system provides quantitative imaging and high precision targeting for the investigation of material properties. Harmonic displacements and harmonic loads were generated during stiffness mapping using the CSM option. In standard applications, the CSM option provides the means for measuring the evolution of mechanical properties as a function of penetration during an indentation test. However, in dynamic imaging the CSM option was used for applying a harmonic displacement oscillation while the tip scanned the surface of the sample and measured the stiffness of the contact to produce a stiffness map of the scanned area.

Two types of tests were conducted to determine the fracture toughness and the scratch parameters of the low k film. Fracture toughness tests were conducted using a diamond cube-corner tip. Cracks were introduced in the film using the indentation cracking method.<sup>1</sup> Quasi-static load-unload tests were performed over 15 seconds with a maximum load of 1.3mN. The cracks produced by the indentation tests were dynamically imaged so that the crack lengths could be accurately measured. Stiffness mapping (a result of dynamic imaging) has shown excellent capabilities in detecting minor fractures and surface abnormalities as compared to standard contact scanning techniques.<sup>2</sup> Dynamic imaging was conducted using a harmonic frequency of 400Hz and a dynamic oscillation of 0.8nm.

Ramp-load scratch testing was also conducted using a cube-corner tip. In a ramp-load scratch test, the tip is brought into contact with the sample; then, the tip is loaded at a constant loading rate while simultaneously translating the sample. Prior to and following the scratch test, a single-line-scan of the surface topography is completed for comparing the original surface to the deformation caused by the scratch test. Therefore, each scratch test consists of three steps: a single-line pre-scan of the area to be scratched, the ramp load scratch test, and a final scan to evaluate the residual deformation. Before and after each step,

a pre-scan and a post-scan, usually equal to 10% or 20% of the scratch length, is performed so that the software can automatically align the data in the three steps. The original and residual single-line scans allow for the evaluation of deformation mechanisms and the quantification of deformation. The scratch process is diagrammed in Figure 1.

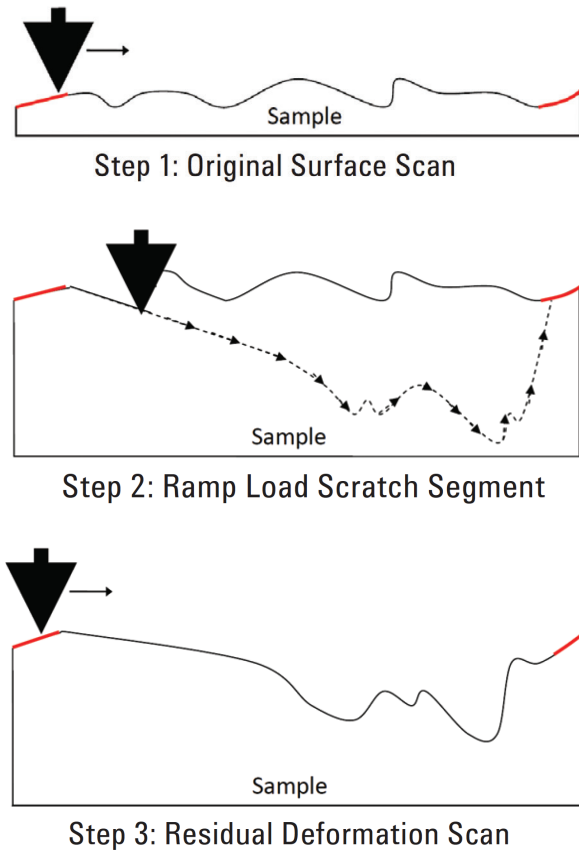


Figure 3. Histogram of one set of 25 indents on sample B'. The median is 2.37GPa; The mean (2.31GPa) is affected by one aberrant indent (H = 0.17 GPa). Histogram is automatically generated by NanoSuite.

When performing scratch testing on any sample set, it is critical that all test parameters and tip geometries remain consistent throughout the samples being compared. This ensures that qualitative comparisons can be made using the resulting data.

The tip chosen for conducting the scratch tests was a cube-corner tip with a tip radius that was, nominally, less than 50nm. A cube-corner tip creates a triangular projected contact with the sample; this tip geometry creates high levels of stress in the material during the scratch. Scratches can be performed either face-forward or edge-forward when using a pyramid shaped indenter. Scratching face-forward with the cube-corner tip acts

like a snow plow and pushes the material out of the way, while edge-forward cuts the material like a knife. A diagram of a cube-corner tip is shown in Figure 2. The low k samples were tested using the cube-corner tip positioned so that it scratched face-forward.

Tests were conducted to a maximum load that continually caused severe failure in the film, which was easily detectable using the resulting scratch curves. To examine the initial location of film failure caused by delamination or blistering, dynamic imaging was used to scan the area around the scratch tests and identify material that had separated from the substrate. Then, the dynamic scan was compared to the 2D scratch curves to identify the finger prints associated with failure.

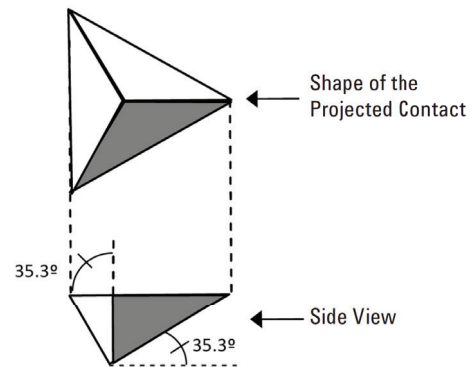


Figure 2. Diagram of cube corner tip.

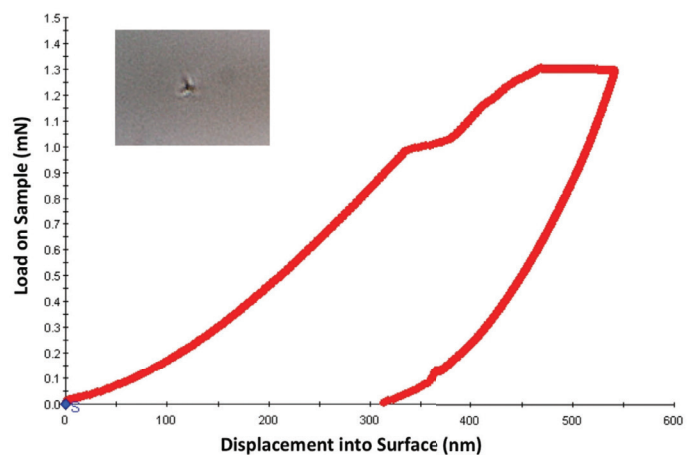


Figure 3. Load-displacement curve of an indentation performed on the low k film to introduce cracking. The residual impression is displayed in the upper-left (1000X magnification).

**Results and Discussion**

Fractures were created in the low k film using a cube-corner indentation tip and performing a quasi-static indentation test up to 1.3mN of force. Fracture of the film can be seen in the load versus displacement curve shown in Figure 3 when the load reached a value of 0.99mN. These cracks continued to propagate as the sample was loaded to 1.3mN—small signs of continued fracture were apparent at forces of 1.16mN and 1.26mN. The residual microscope image, at 1000X magnification, of the indentation test is shown in the upper left corner of Figure 3. While small cracks are apparent, measurements of the crack lengths would not be possible. Therefore, dynamic imaging of the residual indentation was performed to provide a means for measuring the crack lengths in the material without having to transfer the sample to another instrument, such as a scanning electron microscope, for imaging.

One dynamic scan provided the necessary data to produce topography, stiffness, phase angle and harmonic displacement maps of the residual indentation; the four maps are all shown in Figure 4. The topographic map showed evidence of fracture; however, the crack lengths were unclear due to the poor contrast between the large displacement range used in scanning the indent and the small scale displacements seen in fracture. Stiffness, on the other hand, showed much more contrast because only small stiffness changes were apparent due to topographic changes; but, when cracked or blistered material

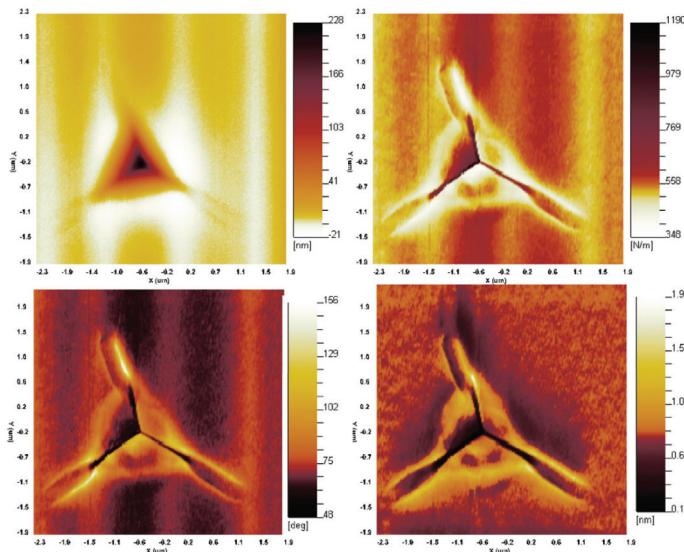


Figure 4. Topography (upper left), stiffness (upper right), phase angle (lower left), and harmonic displacement (lower right) maps of the residual impression left from the indentation test performed in Figure 3. (4.2µm scan)

was encountered, the stiffness changed dramatically. During scanning, when the tip falls into a crack or a sharp edge impression, the contact area increases abruptly and a large stiffness is detected. When the tip has just been removed from a crack or blistered section of the film, the stiffness decreases abruptly due to the limited support of the surrounding material. Dynamic imaging takes advantage of the contrast created when abrupt changes in contact areas are detected. Figure 4 shows that the stiffness and phase angle maps provided the best contrast for measuring the crack lengths. The harmonic displacement map was not used in measuring the crack length because a short lag in harmonic displacement control was apparent after scanning the top crack.

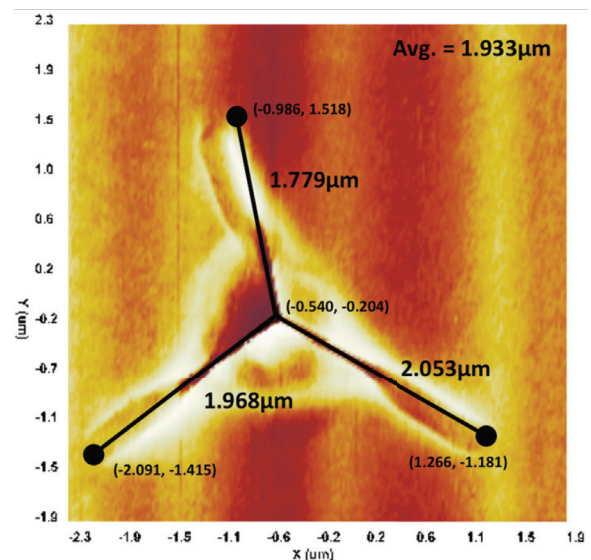


Figure 5. Crack length measurements using the stiffness map produced via dynamic imaging.

Each crack was measured using the stiffness map in Figure 5 and an average crack length of 1.933µm was determined. A first order approximation of the fracture toughness can be determined using the elastic modulus (E) and hardness (H) of the film along with the maximum load (P) and crack length (c) from an indentation test with a cube-corner tip using the relationship in Equation 1.1.

$$K_c = \alpha \left( \frac{E}{H} \right)^{1/2} \left( \frac{P}{c^{3/2}} \right) \tag{Eq. 1.1}$$

Where  $\alpha$  is an empirical constant which depends on the geometry of the indenter—the value of  $\alpha$  for a cube-corner is 0.0319.<sup>1</sup> Values for the elastic modulus and hardness of the film

were determined using the CSM nanoindentation technique described elsewhere.<sup>3</sup> The results for the elastic modulus and hardness of the low k film were  $5.4 \pm 0.1 \text{ GPa}$  and  $0.8 \pm 0.02 \text{ GPa}$ , respectively. The fracture toughness was determined to be approximately  $0.04 \text{ MPa}\sqrt{\text{m}}$ , which is comparable to results reported elsewhere for nanoporous low k films.<sup>4, 5, 6</sup>

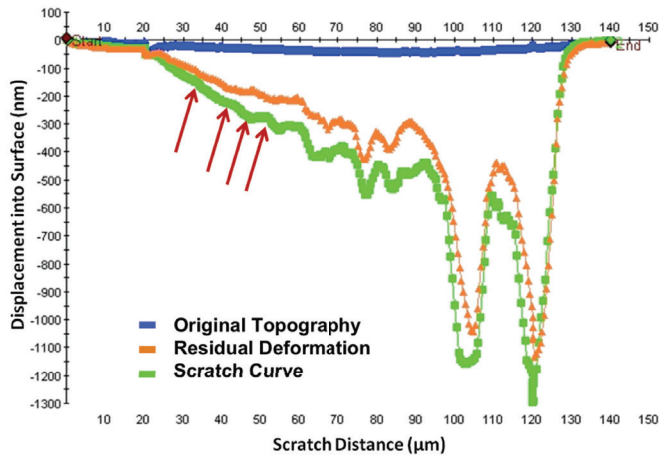


**Figure 6.** The scratch results (original topography, scratch cycle, and residual deformation) from a typical ramp-load scratch test on the low k film using a maximum force of 1mN. Arrows indicate failure in the film.

Scratch testing was conducted on the low k film to better understand failure modes of the film and to better understand separation of the film from the substrate. A ramp-load scratch test to a maximum load of 1mN was used to conduct 100 $\mu\text{m}$ -long scratches. In examination of the resulting scratch curves, multiple points of failure were apparent—the scratch curves for a typical test are shown in Figure 6 with arrows indicating the locations of multiple failure points and possible locations of interface failure. Figure 6 also shows the scans of the original topography (blue), scratch cycle (green), and the residual scan (orange). There was a significant amount of plastic deformation observed in the scratch curves—plastic deformation is depicted by the area between the original topography and the residual deformation, while elastic deformation is depicted by the area between the residual deformation and the scratch cycle—leading up to failure. However, there was insufficient information in the data to decouple deformation mechanisms such as plastic deformation, blistering, and chipping; dynamic imaging of the failure region was used to decouple the three deformation mechanisms and correlate the results to the scratch curves.

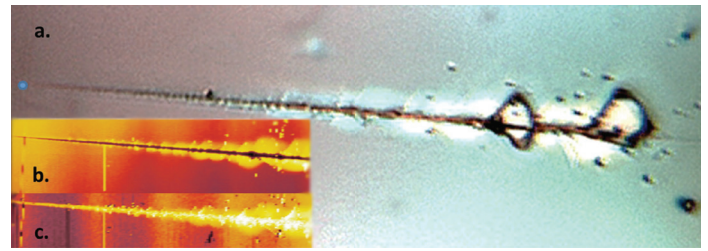


**Figure 7.** Microscope image (a.) of the residual scratch at 1000X magnification aligned with the topography scan (b.) and the stiffness map (c.) of the region of failure.

In Figure 7, the topography scan and stiffness map of the failure region are shown aligned with the microscope image of the residual scratch taken at 1000X magnification; this figure shows that failure of the low k film occurs far before it can be observed in the microscope image. The topography and stiffness maps are shown in greater detail in Figure 8. While the topographical image shows early failure of the film, this failure is dominated by minor pile-up and possibly chipping, which does not classify as interfacial failure. By examination of the stiffness map, clear blistering does not start until a scratch distance of  $52 \mu\text{m}$  is reached; this region is indicated on the stiffness map in Figure 8. Blistering was determined from the stiffness map when the area surrounding the scratch path showed clear radial propagation of low stiffness signifying that the area has separated from other material in the system and was not well supported. The critical load, defined as the first location of delamination or blistering, was located at this point. Figure 9 shows the stiffness map aligned with the scratch data and an arrow indicating the critical load point in the 2D scratch curves.

With the examination of the “finger prints” of failure in the scratch curves, the other scratch data on similar samples were analyzed without the need for imaging. Figure 9 shows that the scratch curve may possess dithers that represent minor chipping of the film—at scratch distances of  $35 \mu\text{m}$  and  $42 \mu\text{m}$  there are noticeable events that occur in the scratch curves—but an arrest of the penetration rate followed by an abrupt acceleration of penetration represented major failure of delamination or blistering in this sample. From analysis of all tests performed on this sample, failure, defined by blistering or delamination, occurred at a normal force of  $0.260 \pm 0.03 \text{ mN}$ .

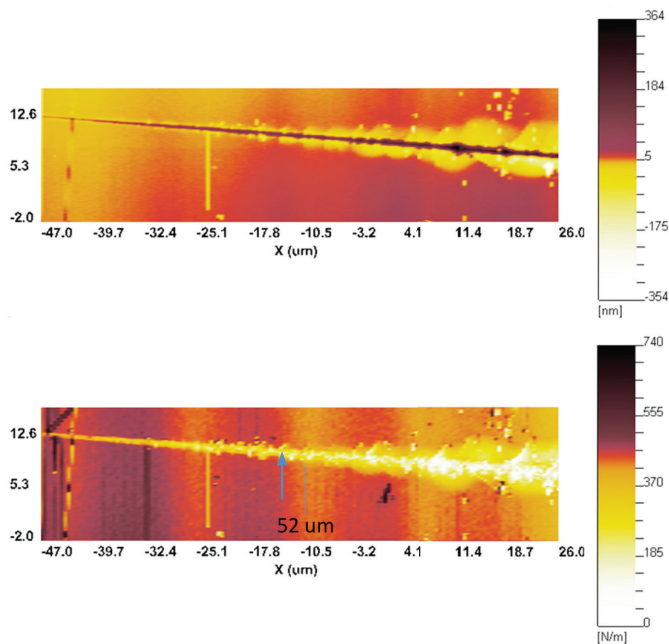


Figure 8. Topography and stiffness maps of the failure region.

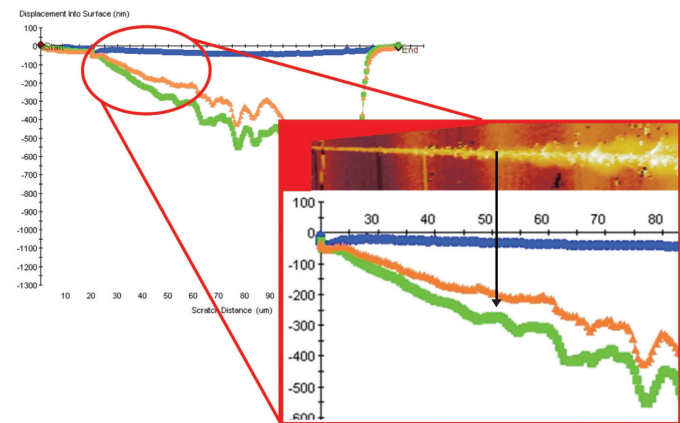


Figure 9. Scratch curves with an outset of the curves aligned with the stiffness map. The arrow locates the finger print of failure that indicates major failure of the film.

**Conclusions**

Dynamic imaging was used to evaluate crack lengths for fracture toughness tests and failure in scratch testing. In examination of the stiffness and phase angle maps, cracks in the low k film were shown to be much longer than could be detected using

topography maps alone. At first inspection, dynamic imaging appears to offer a technique to using a SEM for measuring crack lengths; the result for fracture toughness was comparable to other results obtained using SEM imaging. A larger comparison study should be completed to examine the comparison of crack lengths measured using dynamic imaging and SEM.

Delamination or blistering was apparent in the stiffness map of the scratch test performed on the low k sample. The stiffness map provided the necessary data to identify the finger prints of failure in the 2D scratch curves and use this information to analyze other tests; this is advantageous because the 2D curves take seconds to complete, while stiffness maps require 20 to 45 minutes. Failure of the film was determined by examination of failure that was coupled with a radial propagation of a low stiffness region. While a couple low stiffness areas were observed prior to the area of blistering, these areas were associated with minor failure and pile-up in the film. The use of dynamic imaging allowed observation of failure in indentation and scratch testing that could not be determined through optical microscopy or topography scans.

**References**

[1] Pharr, G.M., Harding, D.S., and Oliver, W.C. "Measurement of fracture toughness in thin films and small volumes using nanoindentation methods." In: M. Nastasi, D.M. Parkin and H. Gleiter Editors, Mechanical Properties and Deformation Behavior of Materials having Ultra-fine Microstructures NATO ASI Series E: Applied Sciences 233 Kluwer, Dordrecht (1993), pp. 449–461.

[2] Crawford, B.A. Stiffness Mapping: a dynamic imaging technique. Keysight Technologies, Inc. application note, 2014.

[3] Oliver, W.C., Pharr, G.M. Measurements of hardness and elastic modulus by instrumented indentation: Advances in understanding and refinements to methodology. Journal of Materials Research, Vol 19, No. 1, Jan 2004.

[4] Morris, D., Cook, R.F. Fracture toughness measurement of thin nanoporous films on stiff substrates. 12th International Conference on Fracture Proceedings, (2009).

[5] Vella, J.B., Adhietty, I.S., Junker, K. and Volinsky, A.A. Mechanical properties and fracture toughness of organo-silicate glass (OSG) low k dielectric thin films for microelectronic applications. International Journal of Fracture 119/120: 487–499, 2003.

[6] Volenskya, A.A., Vellaa, J.B., Gerberich, W. Fracture toughness, adhesion and mechanical properties of low k dielectric thin films measured by nanoindentation. Thin Solid Films 429 (2003) 201–210.

**KLA SUPPORT**

Maintaining system productivity is an integral part of KLA's yield optimization solution. Efforts in this area include system maintenance, global supply chain management, cost reduction and obsolescence mitigation, system relocation, performance and productivity enhancements, and certified tool resale.

© 2019 KLA Corporation. All brands or product names may be trademarks of their respective companies. KLA reserves the right to change the hardware and/or software specifications without notice.

KLA Corporation  
 One Technology Drive  
 Milpitas, CA 95035  
 www.kla.com

Printed in the USA  
 2019-01